

Lab on a Chip

Accepted Manuscript



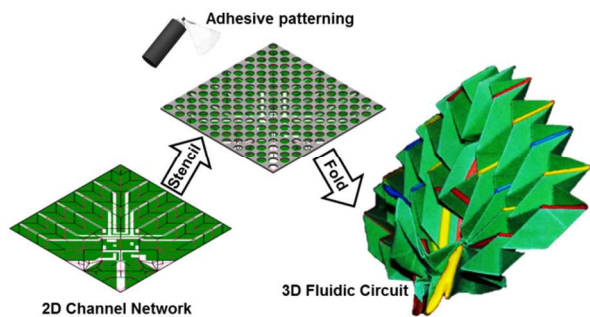
This is an *Accepted Manuscript*, which has been through the Royal Society of Chemistry peer review process and has been accepted for publication.

Accepted Manuscripts are published online shortly after acceptance, before technical editing, formatting and proof reading. Using this free service, authors can make their results available to the community, in citable form, before we publish the edited article. We will replace this *Accepted Manuscript* with the edited and formatted *Advance Article* as soon as it is available.

You can find more information about *Accepted Manuscripts* in the [Information for Authors](#).

Please note that technical editing may introduce minor changes to the text and/or graphics, which may alter content. The journal's standard [Terms & Conditions](#) and the [Ethical guidelines](#) still apply. In no event shall the Royal Society of Chemistry be held responsible for any errors or omissions in this *Accepted Manuscript* or any consequences arising from the use of any information it contains.

This paper details a method of fabricating nonplanar 3D paper microfluidic circuits utilizing patterned aerosol adhesives.



ARTICLE

Patterned Adhesive Enables Construction of Nonplanar Three-Dimensional Paper Microfluidic Circuits[†]

Cite this: DOI: 10.1039/x0xx00000x

Brent Kalish^a and Hideaki Tsutsui^{a,b,c,*}Received 00th January 2012,
Accepted 00th January 2012

DOI: 10.1039/x0xx00000x

www.rsc.org/

This article discusses the fabrication of planar and nonplanar 3D paper microfluidic circuits through the use of patterned spray adhesive application and origami techniques. The individual paper layers are held together via semi-permanent adhesive bonds without the need for external clamps. Semi-permanent bonds accommodate the repeated folding and unfolding required by complex origami device structures and allow the device to be unfolded post-use to view internally displayed results. Combinations of adhesive patterns and fluid channel widths were identified that did not prevent the fluid from traveling between layers and through the entire circuit. Further, this method was extended to nonplanar 3D paper microfluidic circuits, demonstrated via multi-fluid wicking within a modified origami peacock. Such nonplanar 3D paper microfluidic circuits are expected to offer an entirely new platform for exploring new designs and functions of paper analytical devices.

Introduction

Following the development of high resolution fluidic circuits on a cellulose paper substrate in 2007,¹ achieved through the adaptation of photolithographic techniques, the field of paper microfluidics has rapidly expanded in multiple directions, searching for new construction techniques and applications.²⁻⁸ Paper, is defined here to include only cellulose paper, as the proposed methods are not suitable for nitrocellulose membranes, which are insufficiently flexible. Paper has been used as a diagnostic substrate with patterned reaction zones since 1902,^{9,10} with developments in dipstick and lateral flow devices beginning in the 1950s^{10,11} In the last few years, the field of paper microfluidics has been extensively reviewed,^{10,12,13} highlighting the benefits of paper devices, and identifying areas where improvements can yet be made.

Paper devices have a number of advantages over traditional polydimethylsiloxane (PDMS) microfluidic chips, the most prominent being that paper devices do not require an external pump, as all flow is capillary driven. Paper, as a substrate, meets many of the WHO's guidelines for developing diagnostic devices.¹⁴ The guidelines are encapsulated in the acronym ASSURED: Affordable, Sensitive, Specific, User-friendly, Robust and rapid, Equipment-free, and Delivered. Paper devices can easily meet the Affordable and Equipment-free requirements, as paper is a low cost material that is ubiquitous and no external power source or pump is required to wick a fluid through the paper. Depending on the type of analysis being performed, paper pore size, and analyte viscosity, test results can be obtained anywhere from two minutes¹⁵ to one hour¹⁶ and anywhere in between^{3,7,17} meeting the Rapid requirement. On the other hand, paper devices are limited in sensitivity and specificity, due to their qualitative nature of detection methods.

The most common paper microfluidic devices are lateral flow devices.¹⁸⁻²¹ In lateral flow devices, as monolayer devices,

detection can require large footprints⁴, or potentially incompatible additives to adjust fluidic timing as required by more complex detection methods.^{22,23} Multilayer planar 3D devices have attempted to minimize this shortcoming by providing the capability to run multiple independent copies of the same test simultaneously to ensure accuracy or to perform multiple analyses to detect multiple analytes, as multiple channels can pass over one another without mixing.^{2,24,25} Table 1 provides an overview of current 3D microfluidic devices and their method of ensuring interlayer contact. These devices were first constructed of multiple individual paper layers held together with laser-cut double-sided tape.² Each individual layer must be carefully aligned to ensure interlayer fluid transfer. Other devices use liquid adhesives applied between each layer.²⁶ To speed the fabrication process of these types of devices, Lewis et al. developed a technique using an aerosol adhesive to quickly assemble sheets of devices simultaneously.⁸ Most recently, multiple layers of toner from a laser printer, combined with a laminator, has been used to permanently bind multiple, prepatterned paper layers together.²⁷ Alternatively, to avoid any potential adhesive interference, a few groups have explored using origami techniques to fabricate planar multilayer 3D devices out of a single sheet of paper without the use of adhesives; however, such devices require an external clamp to ensure that the layers remain in contact.^{6,28,29} The use of origami folding techniques result in devices that do not require as much time during construction to align sequential layers, because folding along predefined lines will ensure features on adjacent layers are properly aligned. Foldable card devices have also been proposed¹⁶ that include preloaded reagent pads, allowing individuals without extensive training to use the cards, which are activated by folding and adding the sample solution. However, the cards require multiple sheets of different materials and utilize permanent adhesives, preventing the device from being unfolded.

Table 1 Comparison of existing 3D paper microfluidic devices

Authors	Method of Construction	Device Composition	3D Structure	Openable (Unfoldable)
Martinez et al. ²	Double-sided adhesive tape	Individual layers of tape and paper	Planar	No
Govindarajan et al. ¹⁶	Double- and single-sided adhesive tape	Individual layers of tape and paper/polymer	Planar	Yes ⁺
Schilling et al. ²⁷	Laser printer toner	Single sheet of paper	Planar	No
Liu et al. ⁶	External clamps	Single sheet of paper	Planar	Yes
Lewis et al. ⁸	Uniform spray adhesive	Multiple sheets of paper	Planar ⁺⁺	No
Current study	Patterned spray adhesive	Single sheet of paper	Planar Nonplanar	Yes

⁺: Depending on the adhesives, portions of the device may not be openable

⁺⁺: Simple nonplanar devices may be feasible, but have not yet been demonstrated

The current study aims to move a step further by exploring techniques that can be used to create nonplanar 3D circuits, for the first time, using a single sheet of paper, principles of origami, and patterned adhesive application. These techniques result in devices that do not require any additional equipment such as a pump, power source, or clamps, provide greater multiplexing capability,² and can be stored in bulk unfolded before use, or unfolded after use to view test results that are displayed internally, conserving potentially limited analyte volume. Internally displayed results also provide a measure of privacy regarding potentially sensitive results.

Experimental Section

Materials

Allura red, eurioglucine disodium salt, and tartrazine were purchased from Sigma-Aldrich (St. Louis, MO). Whatman grade no. 4 filter paper was purchased from Fisher Scientific (Waltham, MA). Perforated steel sheets were purchased from Metals Depot (Winchester, KY). Super 77 Multipurpose Spray Adhesive (3M, St. Paul, MN) and Repositionable 75 Spray Adhesive (3M, St. Paul, MN) were purchased from McMaster-Carr (Elmhurst, IL).

Test Device Patterning and Fabrication

The test device patterns were designed in SolidWorks (Dassault Systèmes, Vélizy-Villacoublay, FR) and printed onto Whatman grade no. 4 filter paper using a solid wax ink printer (Xerox Phaser 8860).^{30,31} The devices consisted of a circular sample inlet and outlet on the top layer, with a straight channel connecting the two circles on the bottom layer. Devices were designed such that post-melt dimensions would be scaled to the channel width, with channel length measuring 10x its width, surrounded by a wax border as wide as the channel. The paper was then placed on a hotplate for two minutes at 170°C to allow the wax to penetrate vertically through the paper. A spray adhesive was then applied through a stencil, immediately after which the devices were cut out from the sheet, folded in half and compressed between two glass slides by hand. This process is depicted in Figure 1. In addition, a layer of single-sided tape was placed across the bottom of the device to prevent fluid leakage during testing.

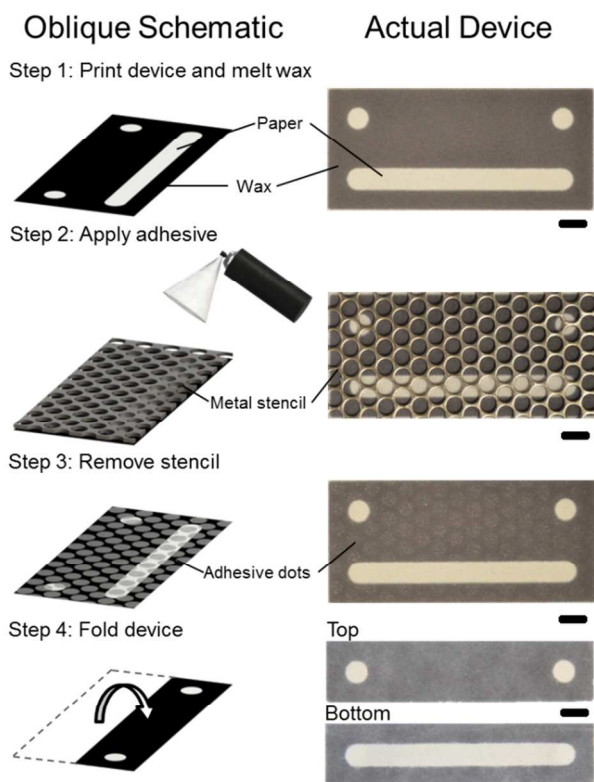


Figure 1 Fabrication process flow of test devices. A sheet of devices is printed onto Whatman grade no. 4 filter paper using a solid wax ink printer. The wax is melted on a hotplate for 2 min at 170°C (Step 1). Upon cooling, a spray adhesive is applied through a stencil made of a perforated steel sheet (Step 2), after which the stencil is removed (Step 3) and the device is cut from its sheet and folded (Step 4). All scale bars are 5 mm.

Adhesive Application

Adhesive was applied from a distance of 24 cm with spray duration of 1 s, with or without a stencil to create a patterned or uniform layer. The stencils were cleaned using adhesive remover after each set of 10 applications to prevent excess adhesive from blocking the stencils' holes. Stencils ranged from 23% open to 63% open with hole sizes ranging from .0625" to .1875". Table 2 lists the details of all the stencils used and depicts the relative hole size differences.

Table 2 1/28" (.91 mm) thick perforated steel sheets used as stencils. All scale bars are 5 mm.

Stencil #	Hole size	Stagger	Percent open	Image
1	1.59 mm (1/16")	3.18 mm (1/8")	23%	
2	2.38 mm (3/32")	3.97 mm (5/32")	33%	
3	3.18 mm (1/8")	4.76 mm (3/16")	40%	
4	4.76 mm (3/16")	6.35 mm (1/4")	51%	
5	3.97 mm (5/32")	4.76 mm (3/16")	63%	

Data Acquisition and Analysis of Test Devices

A green colored solution (10:1 mix of 5 mM tartrazine and 5 mM erioglaucine disodium salt in deionized water) was added to the inlet of each device immediately after device assembly. Ten samples of each channel and stencil combination were tested. Wicking fluid volumes were device dimension specific in order to ensure that devices were not supplied with so much fluid that they could not possibly fail. Fluid volumes are shown in Table 3. Devices were timed until the wicking fluid reached and fully filled the outlet. Devices that did this under the time limit of ten minutes were considered true successes. Devices that did not completely fill the circle or took longer than ten minutes were considered partial successes. The cutoff time of ten minutes was chosen as it was approximately 10x the longest wicking time of the slowest wicking channel without adhesive. Devices that did not have any fluid reach the outlet was considered failures. A depiction of the different success classifications is shown in Figure 2B. Wicking time averages were calculated from only true successes.

Table 3 Fluid amounts used to test each width channel.

Channel Width	Fluid Amount
1 mm	2 μ L
2 mm	7 μ L
3 mm	15 μ L
4 mm	30 μ L
5 mm	50 μ L

Nonplanar Device Design and Construction

The crease pattern used for the nonplanar circuit is based on modified version of Maekawa's³² origami peacock, folded using 15

cm square Whatman grade no. 4 filter paper. The channel pattern is one that allows three distinct channels to pass over one another without mixing. The channel pattern was printed and melted according to the above mentioned methods. The peacock was precreased with a stylus according to the crease pattern before adhesive application. Patterned adhesive was applied through masks in addition to stencil #1 on the front and back of the filter paper. Three colored aqueous solutions (5 mM Allura Red, 5 mM tartrazine, and 5 mM erioglaucine disodium salt) were introduced to the peacock; one to each leg, and the third to a small filter paper lead inserted into the center of the body. The wicking was performed in a sealed chamber containing an open source of water, limiting evaporation. Time lapse images of the wicking process were captured with a Nikon D5100 camera at an interval of 3 minutes between frames.

Results and Discussion

Experimental Design

This paper builds upon separately developed^{6,8} techniques for designing planar 3D paper microfluidic devices, and extends them to create nonplanar 3D devices that do not require external clamps, while still providing the functionality of being able to be unfolded without record destruction. In order to construct nonplanar 3D devices, it was necessary to first develop a method of reliable and rapid interlayer fluid transfer and to ensure that transfer would occur regardless of when the device had been constructed.

An aerosol adhesive was chosen as it significantly reduces device construction time over that required to laser cut double-sided tape and carefully align the layers, as noted by Lewis et al.⁸ They utilized Super 77 Multipurpose Spray Adhesive to provide a permanent bond between device layers. In the present study, as the proposed origami devices require the ability to be unfolded, another adhesive, Repositionable 75 Spray Adhesive was first chosen to be used in the place of the permanent 77.

Repositionable Adhesive

Preliminary testing of the devices, the designs of which are depicted in Figure 2A, involved the application of the spray adhesive 75 without a metal stencil according to the procedure as described by Lewis et al.⁸ (1s spray duration from a 24 cm distance). This resulted in nearly all the devices failing to wick at all, shown in Figure 2C (No Stencil), likely due to 75's spray can having a different nozzle and corresponding spray pattern. Subsequent tests utilized perforated steel sheets to act as stencils, allowing adhesive to be applied to only a portion of the device, limiting potential interlayer interference. Ten samples of each stencil and channel width combination were tested. The results of that testing are also shown in Figure 2C.

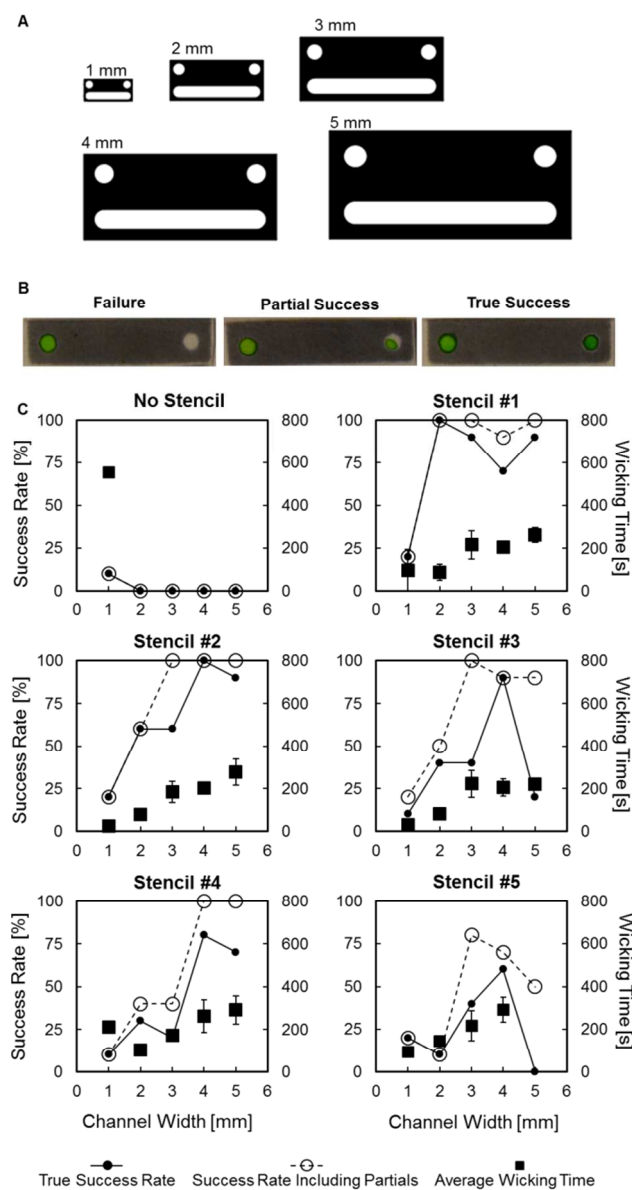


Figure 2 Test device design and performance. A) Devices are all similar in dimensions. The lower channel is 10 times as long as the channel is wide and all borders are designed to be as thick as the channel is wide after melting. B) Device failures are defined as a lack of dye reaching the end. A full success is one in which the outlet circle is completely filled with dye. A partial success is any noticeable amount of dye in the outlet or a full success that took longer than 10 minutes. C) Partial and true success rates (primary axis) for each stencil/channel combination and average wicking times (secondary axis) vs. channel width for devices constructed with adhesive 75 for each of the five stencils and the control, no stencil. N=10. Error bars represent standard deviation.

The 2 mm width channel with stencil #1, the least open stencil (23% open) proved to have shortest wicking time among stencils with a 100% true success rate (Figure 2C). In general, wicking times increased, and success rates fell, as the stencil hole size increased. This is likely due to a higher probability of a stencil hole aligning with the inlet or outlet, resulting in adhesive blocking interlayer flow. Also, in general, increasing the width of the channel increased success rates for most stencils. Further experiments to

determine device lifetime, however, proved that the repositionable adhesive lacked the holding power to extend device viability for much beyond 3 hours, as can be seen in Figure 3A. The device did, however, endure repeated folding while maintaining a high success rate when tested immediately after the repeated folding (Figure 3B).

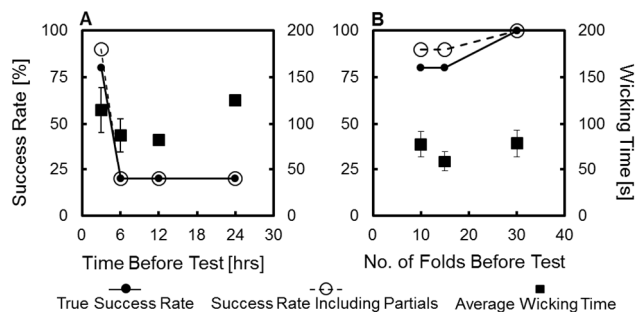


Figure 3 Success rates and average wicking time vs. hours after assembly and vs. repeated folding. A) Device success rate and average wicking time vs. time after device assembly for devices with a 2 mm wide channel and adhesive 75 sprayed through stencil #1. B) Device success rate and average wicking time vs. repeated folds for devices with a 2 mm wide channel and adhesive 75 sprayed through stencil #1. N=10. Error bars represent standard deviation.

Adhesive Comparison

As a result of the lackluster adhesion of the repositionable adhesive (i.e. the 75), a test was designed to compare the relative strengths of the 75 and the 77. The 75's tack range extends into the hours, which allows the device to be folded into complex shapes that required repeated contact of adhesive bearing surfaces; however this impermanent bond allows the paper to unfold itself over time. The 77, as a permanent adhesive, only remains tacky for up to 30 minutes, yet long enough for device construction and thought to be unlikely to allow the layers to separate. A checkerboard wax pattern (to provide contrast) was printed, melted and sprayed with both adhesives. The adhesives were applied both with and without a stencil. The papers were folded and compressed, as with previous tests, and left to sit for 3 hours, after which they were unfolded (Figure 4). As expected, when applied without a stencil, the repositionable 75 was able to be unfolded without tearing the paper, while with the permanent 77 the paper was torn in half (Figure 4A). However, when applied through stencil #1, the 77 performed comparably to the 75, as both were able to be unfolded with ease (Figure 4B).

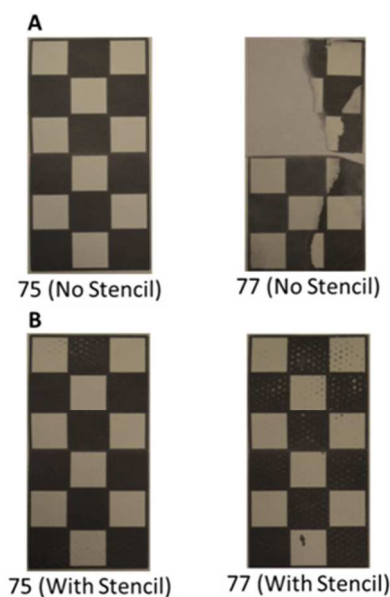


Figure 4 Peel test comparison of adhesive 75 (Left) and adhesive 77 (Right) 3 hours after adhesive application. A) Adhesive application without a stencil. B) Adhesive application through stencil #1. As expected, without a stencil, adhesive 75 was able to be unfolded without tearing the paper, while adhesive 77 suffered extensive paper damage. However, when applied through stencil #1, both adhesives performed comparably, unfolding with ease. The peel test strips are 60 mm wide and 120 mm long while unfolded.

Permanent Adhesive

In light of these results, it was proposed that we repeat the channel and stencil tests now with the permanent adhesive 77 in order to identify a channel and stencil combination that would result in devices that had the shortest wicking time in addition to a high success rate. The results of those tests are shown in Figure 5.

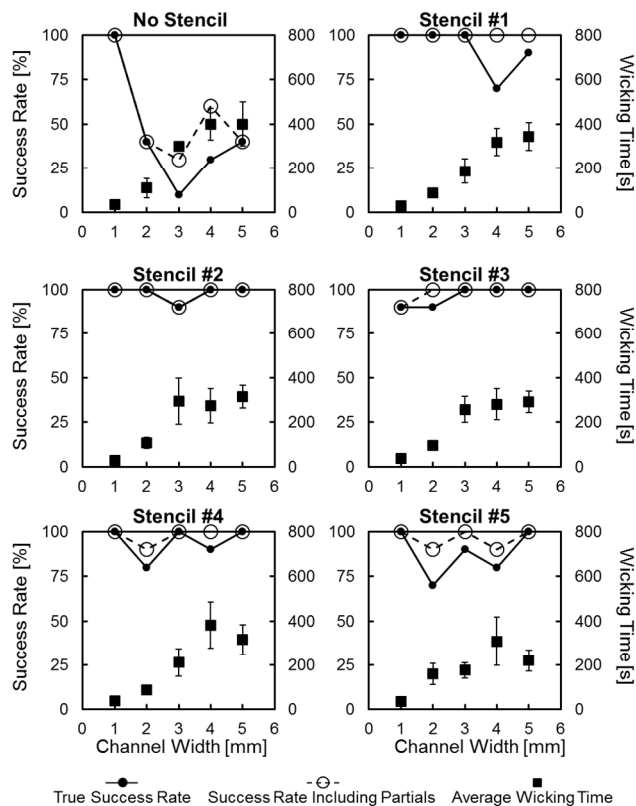


Figure 5 Partial and true success rates (primary axis) for each stencil/channel combination and average wicking times (secondary axis) vs. channel width for devices constructed with adhesive 77 for each of the five stencils and the control, no stencil. N=10. Error bars represent standard deviation.

While devices constructed with 77 had somewhat slower wicking times than those of their 75 counterparts, they all had much higher success rates. As with the 75, 77 applied through stencil #1 resulted in devices with standard deviations that were among the lowest out of all channel/stencil combinations. All devices constructed with stencil #1 had a 100% partial success rate, indication that by increasing wicking fluid volume, 100% true success rates would be achievable.

A brief study was performed on 2 mm wide channels to determine the effect of spray adhesives on wicking times in a 1D channel (Figure S1, ESI[†]). Uniform adhesive coverage resulted in much slower wicking in adhesiveless channels, with 77 coated channels wicking even slower than in 75 coated channels. This agrees with the data obtained from the folded device wicking, in which devices constructed with 77 took longer to wick than those constructed with 75. Both sets of adhesive-covered channels wicked the full length of their channels, unlike with the folded 2 mm devices. When applied through stencil #1, both adhesives had comparable wicking times that fell in-between the wicking times of the adhesiveless 1D channel and the folded devices. The results of this study suggest that inhibited interlayer transfer contributes to diminished wicking success rates and increased wicking times. The full results of this study are shown in Figure S1 (ESI[†]).

As with the 75, we wanted to confirm that the devices would still remain viable for extended periods of time after device construction, while still retaining the ability to be folded and unfolded repeatedly, like devices constructed with the 75. These tests were performed with the 2 mm channel devices,

despite having a slower wicking speed than the 1 mm channel, because the 1 mm channel devices were too small to easily manipulate for the required number of folds. Additionally, the dimensions of the 1 mm channel device approach the functional channel width limit obtainable with wax printing methods.³¹ The 2 mm channel also had a much smaller deviation in wicking times than the larger channels. As shown in Figure 6A, the 77 was able to maintain device viability for all ten samples for at least 24 hours after device construction. Devices constructed with 77 were able to be folded just as many times before being tested, as shown in Figure 6B. Testing was performed immediately following the repeated folding, while still within the 77's tack range.

Further device viability studies were conducted to determine the effect of ambient humidity on the adhesive's ability to maintain interlayer contact (Figure S2). 2 mm devices with adhesive applied through stencil #1 were stored for a week in containers filled with air of different relative humidity levels or dry nitrogen. After one week, devices were tested. Success rates fell as relative humidity levels increased, with the highest success rates (90%) found when devices were stored under dry nitrogen. Such a storage condition, under dry inert gas, is a standard packaging practice for many medical devices and sensitive biological reagents. For longer term storage, or storage under non-ideal conditions, other adhesives (eg. non-hygroscopic) may prove to be more advantageous.

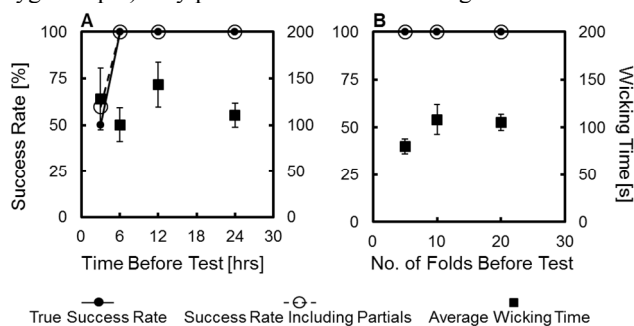


Figure 6 Success rates and average wicking time vs. hours after assembly and vs. repeated folding. A) Device success rate and average wicking time vs. time after device assembly for devices with a 2 mm wide channel and adhesive 77 sprayed through stencil #1. B) Device success rate and average wicking time vs. repeated folds for devices with a 2 mm wide channel and adhesive 77 sprayed through stencil #1. N=10. Error bars represent standard deviation.

Nonplanar Devices

In order to expand the technique of patterned adhesive application beyond planar devices, a nonplanar 3D origami structure was chosen to serve as a proof concept. A nonplanar structure would be crushed by the use of any sort of external clamp and the folding order of origami precludes uniform application of a permanent adhesive, because latter steps require unfolding previously made folds. The fluidic circuit within the core of the chosen origami structure was designed using the newly obtained knowledge of adhesive application patterns. The base origami design is a modified version of Maekawa's³² peacock (Figure 7A). Spray adhesive 77 was applied through stencil #1 (23% open), the stencil that applied the least amount of adhesive in previous tests. A pair of masks were used to apply the patterned adhesive to specific portions of each side of the precreased peacock in order to minimize

excess adhesive interfering with folding (Figure 7B). As shown below in Figure 7C and 7D, three distinct colored fluids were able to wick through the peacock's channels and pass over one another inside the body region without mixing. The callout in Figure 7D shows the direction of blue, yellow, and red solution transport through 3 folded layers without mixing, connecting to three, four, and four channel branches, respectively. A video (Video S1, ESI[†]) made from time lapse images of this test is available in the Electronic Supplementary Information.

Beyond demonstrating interlayer fluid transfer in a nonplanar 3D structure, the tail of the peacock demonstrates the ability for wicking driven actuation. As the fluid wicks through symmetrically distributed channels, the tail is forced open (Figure 7C). This opening arises from liquid wicking across folds, where swelling cellulose fibers force open the folds. In addition, the weight of the wicking fluid as it extends outward along the tail, may serve to pull the sides of the tail downwards. These two forces, when coupled with an elastomeric film,³³ could form an actuator powered by a fluid wicking along a channel and across strategically placed folds. Once the wicking fluid evaporates, the device would be able to return to its previous configuration. Similar behavior is found in nature, where some seeds (eg. *Pelargonium carnosum*), utilize changes in atmospheric humidity to propel themselves into the ground³⁴. During periods of low atmospheric humidity, the seed's awn (a seed's fibrous "tail") will dry out, forming a coil, and once atmospheric humidity increases, the hygroscopic awn will straighten out, propelling itself into the ground. It is anticipated that nonplanar 3D paper microfluidic techniques can enable the mimicry of some of nature's designs and functions in novel paper microfluidic devices.

Conclusions

This work demonstrates how the use of patterned adhesives enables the construction of nonplanar 3D paper microfluidic circuits. To the best of our knowledge, this is the first demonstration of a nonplanar 3D origami paper microfluidic circuit with interlayer fluid transport (Table 1). Current origami microfluidic devices are planar structures and thus require either external clamps, or the use of multiple paper layers and permanent adhesives to ensure interlayer fluid transfer. Origami devices⁶ constructed with aerosol adhesives⁸ benefit from a greatly reduced assembly time and the use of a stencil minimizes the amount of adhesive applied, limiting potential adhesive interaction with the wicking fluid (Figure S1, ESI[†]). Minimal adhesive covering with a permanent adhesive such as the Super 77 Multipurpose Spray Adhesive results in semi-permanent bonds between paper layers. Such bonds allow repeated folding and unfolding, enabling devices to be unfolded after use, or during assembly to enable more complex folding without tearing. Additionally, the lack of external clamps enables the construction of nonplanar 3D devices that can be used to perform tasks that would otherwise be impossible in a planar structure. For example, elastomeric films could be combined with nonplanar paper microfluidic devices to form diagnostic devices capable of actuation powered by fluid wicking within the device. Alternatively, these techniques could couple diagnostic capabilities to existing actuators, in particular, pneumatic actuators formed from cellulose paper embedded into elastomer matrices.³⁵ Such devices take advantage of origami folding principles to increase their stiffness and anisotropy of their actuation. As modern origami art has evolved into truly complex 3D folding,³⁶ paper

diagnostic devices are likely to benefit from such creative folding, enabling previously unaccomplished functions.

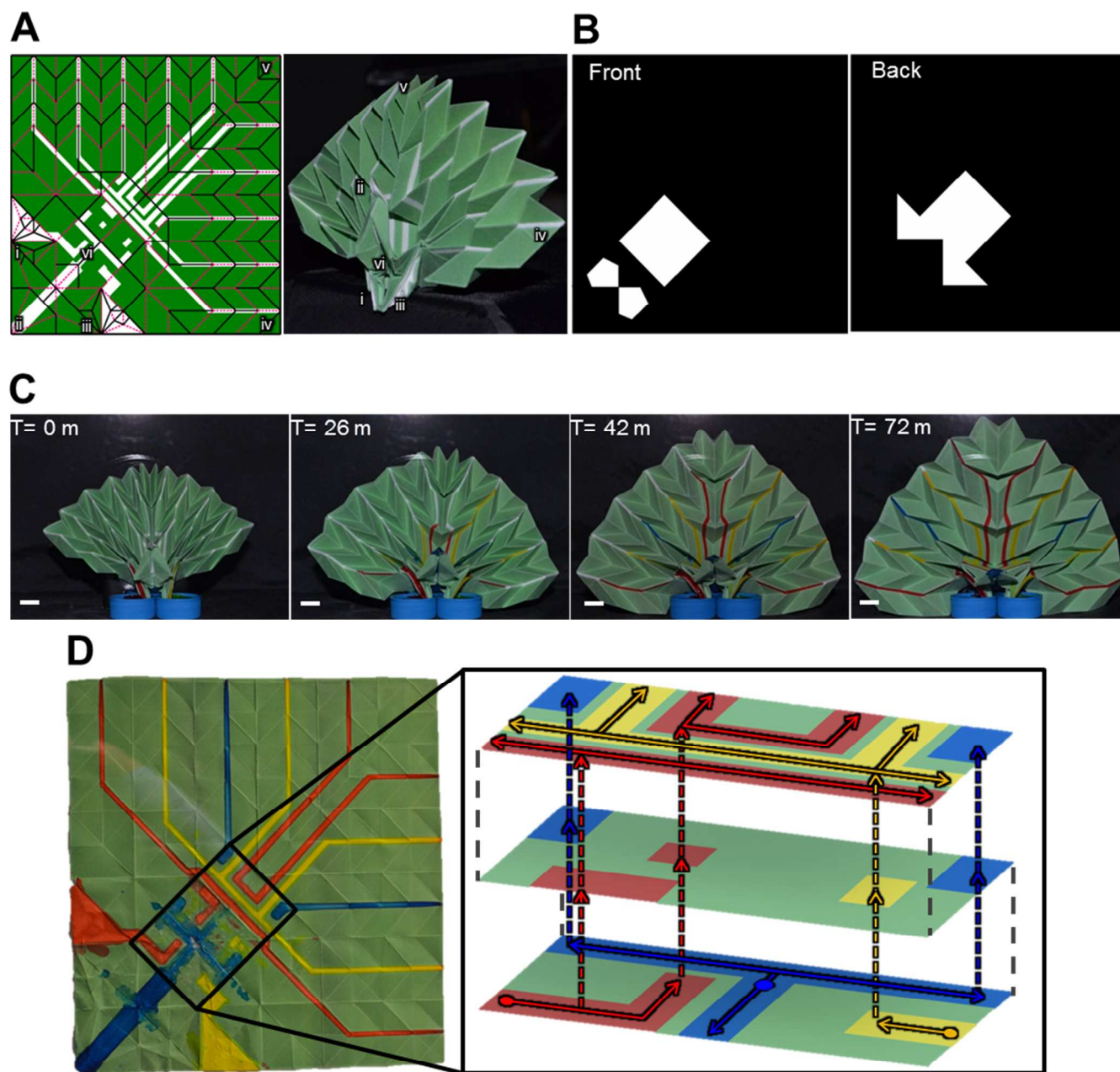


Figure 7 Nonplanar origami circuit design and performance. A) Peacock crease pattern modified from Maekawa's origami design overlaid on the wax boundary regions. Dotted red lines correspond to mountain folds, while solid black lines are valley folds. Roman numerals i-vi indicate identical points before and after folding: (i) right leg where red dye is introduced, (ii) head, (iii) left leg where the yellow dye is introduced, (iv) left-most point of the tail, (v) top of the tail, and (vi) center of the body, to which a leader is attached to introduce the blue dye. B) Masks to limit adhesive application to certain regions of peacock: Front (left) and Back (right) masks. White regions correspond to areas where patterned adhesive was applied. C) Time lapse of fluid wicking through the peacock. Colored water was wicked through each leg and a 5 mm wide filter paper leader to the main body. Wicking took place in a sealed chamber with an open pool of water to simulate a high relative humidity. Wicking time took approximately 2 hours. Video S1 is available in ESI[†] Scale bars are 1 cm. D) Unfolded peacock post-wicking with a schematic view of how the channels connect when folded. The three colored solutions (Red – allura red, Blue – erioglaucine disodium salt, Yellow - tartrazine) can be seen to have not mixed either inside or outside of the channels in the unfolded peacock. In the callout

schematic, dotted gray lines indicate a continuation of paper over folds. Inlets are marked by circles. Arrows indicate direction of flow

Acknowledgements

This work is supported by an initial complement fund from Bourns College of Engineering of University of California, Riverside.

Notes and references

^a Department of Mechanical Engineering, University of California, Riverside, Riverside, CA 92521, USA. Email: htsutsui@engr.ucr.edu

^b Department of Bioengineering, University of California, Riverside, Riverside, CA 92521, USA.

^c Stem Cell Center, University of California, Riverside, Riverside, CA 92521, USA.

†Electronic Supplementary Information (ESI) available: Time lapse video of nonplanar 3D paper microfluidic wicking and additional figures. See DOI: 10.1039/b000000x/

- A. W. Martinez, S. T. Phillips, M. J. Butte and G. M. Whitesides, *Angewandte Chemie*, 2007, 46, 1318-1320.
- A. W. Martinez, S. T. Phillips and G. M. Whitesides, *Proceedings of the National Academy of Sciences of the United States of America*, 2008, 105, 19606-19611.
- C. M. Cheng, A. W. Martinez, J. Gong, C. R. Mace, S. T. Phillips, E. Carrilho, K. A. Mirica and G. M. Whitesides, *Angewandte Chemie*, 2010, 49, 4771-4774.
- E. Fu, S. A. Ramsey, P. Kauffman, B. Lutz and P. Yager, *Microfluidics and nanofluidics*, 2011, 10, 29-35.
- A. W. Martinez, S. T. Phillips, Z. Nie, C. M. Cheng, E. Carrilho, B. J. Wiley and G. M. Whitesides, *Lab on a chip*, 2010, 10, 2499-2504.
- H. Liu and R. M. Crooks, *Journal of the American Chemical Society*, 2011, 133, 17564-17566.
- C. Renault, X. Li, S. E. Fosdick and R. M. Crooks, *Analytical chemistry*, 2013, 85, 7976-7979.
- G. G. Lewis, M. J. DiTucci, M. S. Baker and S. T. Phillips, *Lab on a chip*, 2012, 12, 2630-2633.
- United States of America Pat.*, 691,249, 1902.
- A. K. Yetisen, M. S. Akram and C. R. Lowe, *Lab on a chip*, 2013, 13, 2210-2251.
- A. H. Free, E. C. Adams, M. L. Kercher, H. M. Free and M. H. Cook, *Clinical chemistry*, 1957, 3, 163-168.
- X. Li, D. R. Ballerini and W. Shen, *Biomicrofluidics*, 2012, 6, 11301-1130113.
- V. Gubala, L. F. Harris, A. J. Ricco, M. X. Tan and D. E. Williams, *Analytical chemistry*, 2011, 84, 487-515.
- H. W. Kettler, Karen; Hawkes, Sarah, in *Mapping the landscape of diagnostics for sexually transmitted infections*, World Health Organization, Geneva, SW, 2004, pp. 1-37.
- Y. K. Oh, H. A. Joung, S. Kim and M. G. Kim, *Lab on a chip*, 2013, 13, 768-772.
- A. V. Govindarajan, S. Ramachandran, G. D. Vigil, P. Yager and K. F. Bohringer, *Lab on a chip*, 2012, 12, 174-181.
- S. J. Vella, P. Beattie, R. Cademartiri, A. Laromaine, A. W. Martinez, S. T. Phillips, K. A. Mirica and G. M. Whitesides, *Analytical chemistry*, 2012, 84, 2883-2891.
- C. Danks and I. Barker, *EPPO Bulletin*, 2000, 30, 421-426.
- D. Y. Stevens, C. R. Petri, J. L. Osborn, P. Spicar-Mihalic, K. G. McKenzie and P. Yager, *Lab on a chip*, 2008, 8, 2038-2045.
- D. M. Cate, W. Dungchai, J. C. Cunningham, J. Volckens and C. S. Henry, *Lab on a chip*, 2013, 13, 2397-2404.
- R. Chen, H. Li, H. Zhang, S. X. Zhang, W. M. Shi, J. Z. Shen and Z. H. Wang, *Anal Bioanal Chem*, 2013, 405, 6783-6789.
- B. Lutz, T. Liang, E. Fu, S. Ramachandran, P. Kauffman and P. Yager, *Lab on a chip*, 2013, 13, 2840-2847.
- H. Noh and S. T. Phillips, *Analytical chemistry*, 2010, 82, 4181-4187.
- L. Ge, J. Yan, X. Song, M. Yan, S. Ge and J. Yu, *Biomaterials*, 2012, 33, 1024-1031.
- M. Zhang, L. Ge, S. Ge, M. Yan, J. Yu, J. Huang and S. Liu, *Biosensors & bioelectronics*, 2013, 41, 544-550.
- L. Ge, S. M. Wang, X. R. Song, S. G. Ge and J. H. Yu, *Lab on a chip*, 2012, 12, 3150-3158.
- K. M. Schilling, D. Jauregui and A. W. Martinez, *Lab on a chip*, 2013, 13, 628-631.
- K. Scida, B. Li, A. D. Ellington and R. M. Crooks, *Analytical chemistry*, 2013, 85, 9713-9720.
- J. Yan, M. Yan, L. Ge, J. Yu, S. Ge and J. Huang, *Chemical communications*, 2013, 49, 1383-1385.
- Y. Lu, W. Shi, L. Jiang, J. Qin and B. Lin, *Electrophoresis*, 2009, 30, 1497-1500.
- E. Carrilho, A. W. Martinez and G. M. Whitesides, *Analytical chemistry*, 2009, 81, 7091-7095.
- J. Maekawa, *Genuine Origami: 43 Mathematically-Based Models, From Simple to Complex*, 2008.
- R. Kempaiah and Z. H. Nie, *J Mater Chem B*, 2014, 2, 2357-2368.
- W. Jung, W. Kim and H. Y. Kim, *Integrative and comparative biology*, 2014, DOI: 10.1093/icb/ucu026.
- R. V. Martinez, C. R. Fish, X. Chen and G. M. Whitesides, *Adv Funct Mater*, 2012, 22, 1376-1384.
- R. J. Lang, *Origami Design Secrets: Mathematical Methods for an Ancient Art*, 2nd edn., 2011.